Advances in Applied Energy 17 (2025) 100208

Contents lists available at ScienceDirect

Advances in Applied Energy

journal homepage: www.elsevier.com/locate/adapen

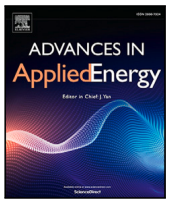

Integrating water availability for electrolysis into energy system modeling

Julian Walter [a,*], Lina Fischer [a], Sandra Venghaus [b,c], Albert Moser [a]

[a] Institute for High Voltage Equipment and Grids, Digitalization and Energy Economics, RWTH Aachen University, Schinkelstr. 6, Aachen, 52062, Germany
[b] Decision Analysis and Socio-economic Assessment, School of Business and Economics, RWTH Aachen University, Kackertstr. 7, Aachen, 52072, Germany
[c] Institute of Climate and Energy Systems - Jülich Systems Analysis, Forschungszentrum Jülich, Wilhelm-Johnen-Str., Jülich, 52428, Germany

ARTICLE INFO

Keywords:
Energy system optimization model
Integrated energy system
Energy system planning
Water availability
Electrolysis
Hydrogen

ABSTRACT

In recent years, temperature records have been broken all over the world and the global temperature keeps rising. As a result, fresh water availability will diminish ever more and more due to droughts and extreme weather events. Water is a key part of many central aspects of life but will also become important in the future for electrolysis to synthesize hydrogen, a promising energy carrier in energy systems for the transition from fossil to renewable energy. Current energy system optimization models neglect water as an input for electrolysis when focusing on electricity. In this study, we present a method for implementing water as an input in energy system optimization models, with constraints for freshwater availability and seawater processing. We apply our method to one scenario and investigate the impact on the European energy system with highly-detailed spatial and temporal resolutions. The results indicate a relocation of electrolysis capacities of 10% and an increase of methane imports and methanation capacities. The effects suggest that water should be considered in energy system optimization in the future.

1. Introduction

For the Paris Climate Agreement of 2015, 195 countries signed on to action to mitigate climate change and keep the increase in global surface temperature below 2 °C [1]. Therefore, the European Union set itself the goal within the European Green Deal to become climate-neutral by 2050 [2]. To achieve this, a fundamental transformation of the energy system is necessary. One promising solution is the development of a sector-integrated energy system that comprises various energy carriers, their transport and plant infrastructure as well as sector-coupling technologies that link the energy carriers together. The most energy-efficient option to reduce greenhouse gas emissions in the energy system and applications is to use electricity from renewable sources directly whenever possible [3–5]. For applications where direct electrification is not possible, synthetic hydrogen produced from renewable electricity and water via electrolysis plays a major role [6–8]. Hydrogen derivatives, such as synthetic methane and, e.g., Fischer–Tropsch fuels, are also widely discussed [9–11].

Energy system optimization models (ESOMs) are used to investigate future energy system designs. Given their capacity to derive infrastructure needs while incorporating interdependencies between energy carriers, power plants, and energy transport, they are often used for policy-making. There is already a broad array of ESOMs, once classified by Prina et al. [12] and Lopion et al. [13] regarding their resolution, trends and challenges. Some of these models, e.g., BALMOREL [14], LUT [4,9], PyPSA-Eur [15], GENESYS-MOD [16] and others have detailed spatial and temporal resolutions [17–20]. Some of these models, e.g., PyPSA [21], eMix [22], PRIMES [23], LISA [24] are techno-economically wise detailed, and some, e.g., REMIX [25], PyPSA-Eur-Sec [26], LEGO [27], and others integrate more energy carriers and their infrastructures [12,13,28]. Oftentimes, these models are adjusted to answer a particular research question. Some of these models were already used specifically to research coupled electricity and hydrogen infrastructures. Klatzer et al. modeled in detail the expansion and operation of hydrogen transport infrastructures in coupled energy systems [29]. In their study, Brown et al. examined the sectoral interactions between electricity, hydrogen, and gas in a European energy system of 30 nodes [30]. The potential for hydrogen and its import dependency in an integrated European energy system was part of an investigation by Blanco et al. [10].

However, all of the models and studies known to the authors only consider electricity as an input for electrolysis. None of them generally integrate water as an input for electrolysis and, respectively, as a limited resource, even though it is a crucial resource to many aspects of life. Its absence or scarcity can lead to severe problems. In Europe, there are already regions experiencing aridity and water stress and it is expected that ongoing climate change will lead to further changes in

* Corresponding author.
E-mail address: julian.walter@rwth-aachen.de (J. Walter).
URL: https://www.iaew.rwth-aachen.de (J. Walter).

https://doi.org/10.1016/j.adapen.2025.100208
Received 22 November 2024; Received in revised form 4 January 2025; Accepted 7 January 2025
Available online 27 January 2025

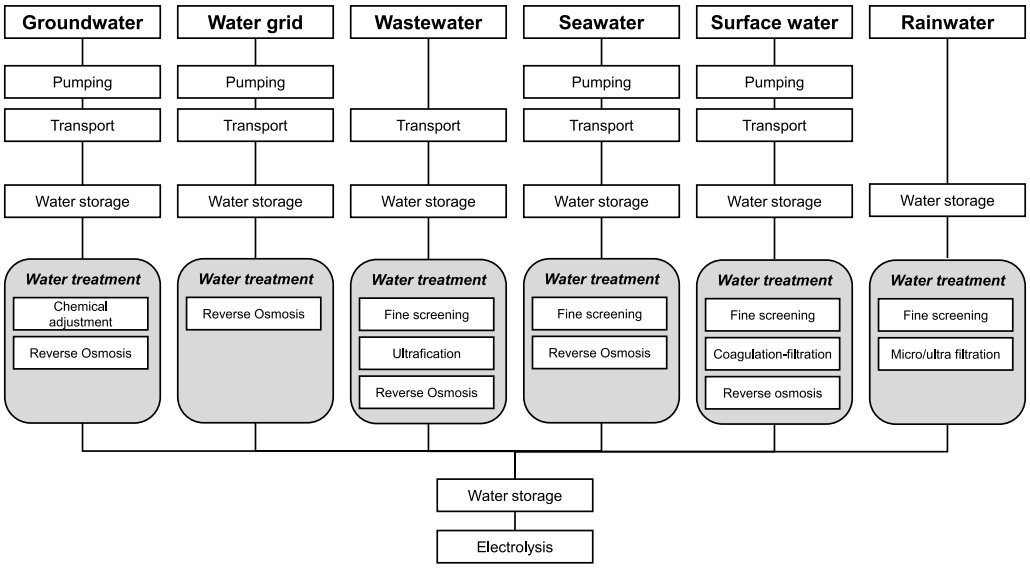

Fig. 1. Water sources and processing for electrolysis [36].

availability and competition for available water [31]. A rapid increase in water stress is predicted in the coming years, for example in the Mediterranean regions [31]. These changes could result in more European regions facing severe water stress and limited water availability. Although only 9–11 liters of freshwater are necessary to synthesize 1 kWh of hydrogen, recent years have shown that climate change creates ever more and more droughts and freshwater availability to decrease. At a certain point, any further water extraction could evoke serious negative long-term and cascading ecological, economical, and social effects. In ecological terms, limited water availability and water stress can cause a decline in water quantity, e.g., dry rivers or water shortages, and water quality, e.g., organic matter pollution or saline intrusion [32]. In economical terms, it prevents industrial, urban, and tourism development [33]. In social terms, it can cause food insecurity, a diminution of basic hygiene, and health issues such as increased the likelihood of water-, food-, and vector-borne diseases [34]. Studies have also shown that water scarcity can triple the local likelihood of social conflicts [35]. As fresh water is a necessary feedstock for producing hydrogen via electrolysis, and all additional water extraction in regions with water stress increases the stated problems, limited water availability is a crucial constraint when determining locations for electrolysis from an overall system perspective. Processing seawater for use in electrolysis is another, but more expensive, possibility that will tend to make locations with electrolysis capacities to coastal regions and not interfere with fresh water availability. Adding these constraints to ESOMs will likely change the results in favor of more resource-efficient locations for electrolyzers not affecting water stress and subsequent consequences in comparison to ESOMs' results without constraints for limited water availability and water as an input for electrolysis.

Some studies have investigated the development of freshwater availability in Europe under encroaching climate change. Due to the great importance of water in many central aspects of life and the predicted changes associated with limited water availability, the development of water resources and water stress are the subject of current research, as in [37–39], and [40]. Other studies researching interactions within the food energy water nexus on a more global level do not examine their research question in the context of energy system or location planning for electrolyzers [41–43].

It has become clear that the development of water availability is a very important issue to consider. Yet in the fields of ESOMs and energy system planning, where electrolysis based on RES and water plays a pivotal role [29], water as a limited resource and input for electrolysis has been left untouched thus far. We considered how the implementation of this into ESOMs is possible and what impacts this may have on energy system optimization results, especially in locations for electrolysis and RES. We therefore extend an existing ESOM with constraints modeling regional limited fresh water and unlimited seawater availability, as well as the necessary water processing for both fresh and seawater. Furthermore, we added constraints and variables for modeling water as an input for hydrogen production via electrolysis. Finally, we compared two scenarios, one without the added constraints and one with integrated constraints with regard to locations for electrolysis capacities and the import of hydrogen, methane, and liquid fuels.

The paper is structured as follows: in Section 2, we analyze water sources for electrolysis and the general development of water availability. In Section 3, the implementation of water availability water as an input in the existing ESOM is described. Section 4 presents the scenario, including the temporal and spatial resolutions, as well as the results of the conducted studies. Two scenarios for the year 2050, one without and one including future water availability, are investigated to elaborate on the research question. Finally, Section 5 discusses the results, the developed approach and briefly summarizes the main findings of the conducted investigations.

2. Background

In order to investigate the impact of water used for electrolysis in the future energy system, we first examine water sources and their availability. In [36], Simoes et al. researched water sources, together with their treatment needs for hydrogen production. Freshwater electrolysis requires clean and deionized water as an input. The possible water sources differ mainly in terms of their level of pollution and thus the processes necessary for their treatment (see. Fig. 1).

Of the water sources noted in Fig. 1, groundwater usually provides water of good quality, with the soil playing a crucial role in the water filtering of it [36]. However, the continuous availability of groundwater is questionable, and significant pumping efforts may be necessary to access it. As an alternative source, water grids also offer good water quality, but large-scale supply to electrolysis could overload the water grid. Moreover, water use for electrolysis would compete with concurrent water uses such as human consumption [36]. Industrial and urban wastewater is already processed and polluted by preceding processes, which makes additional wastewater treatment necessary [36]. In addition to that, the large-scale availability of wastewater is uncertain. The supply of rainwater is difficult to forecast and significant collection and storage facilities must be built in order to utilize it [36]. These costs

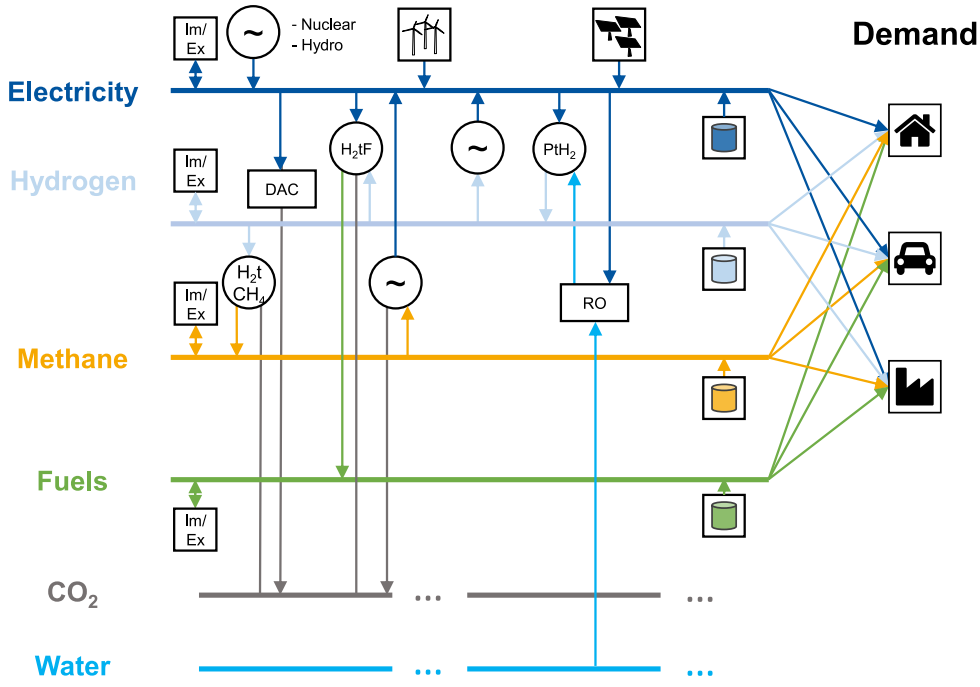

Fig. 2. Overview technological system area.

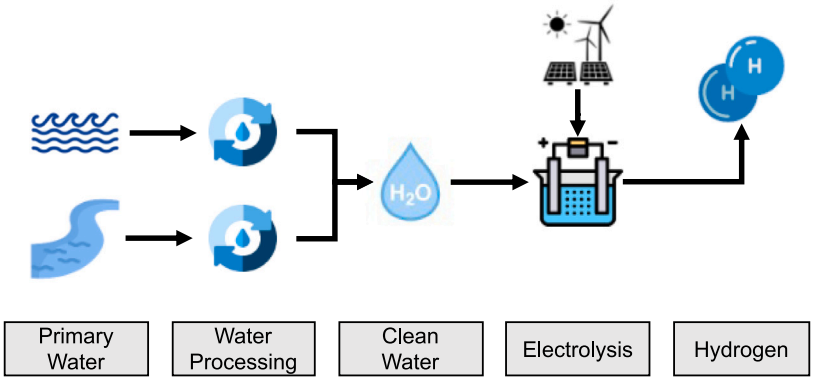

Fig. 3. Approach to water processing in energy system optimization models.

question the feasibility of rainwater for electrolysis, even though little processing must be performed. Surface water covers rivers, streams, and lakes and typically offers good water quality. However, the availability of surface water underlies seasonal variances [36]. Seawater, on the other hand, needs more complex and expensive treatment but provides a water supply with good availability and reliability [36]. Taken together, the water sources differ in their suitability for electrolysis. In particular, its availability for large-scale electrolysis of groundwater, water from water grids, wastewater, and rainwater, is questionable. Therefore, in the context of this paper, we only consider surface water and seawater, as these are highly available water sources.

Although the extent of water treatment depends on the water source (see. Fig. 1), all sources except rainwater have the process of reverse osmosis (RO) in common [36]. For surface water and seawater, additional water treatment steps include fine screening and coagulation-filtration [36]. Of these, RO is the most energy-intensive step in the process chain and entails the most water losses, the exact efficiency depending on the composition of the water source though [36]. In comparison, fine screening and coagulation filtration only cause negligible water losses and energy demands and are therefore not decisive processes within the scope of this paper [36]. Hence, we only consider reverse osmosis as a decisive process step to implement in the model.

Although seawater is a more or less unlimited resource, freshwater from surface water is limited. Although water consumption for global hydrogen production could be covered using only about 0.00015% of the world's freshwater resources, the water's availability is highly dependent on the region [38]. Regional differences can be caused by significantly varying water usage (e.g., from agriculture or other water-dependent sectors), climatic conditions, or the shape of watercourses [39]. In 2020, the European Commission analyzed the impact of climate change on the water supply in Europe and predicted that regions around the Mediterranean Sea would experience less freshwater availability, whereas its availability in northern European regions is not likely to change or even increase [11].

The Water Exploitation Index (WEI) is a way to proportion freshwater availability. The WEI is the ratio of available freshwater divided by annual freshwater consumption. The index is often used as a way to define water stress, with water stress causing "... deterioration of fresh water resources in terms of quantity [...] and quality [...]", according to the European Environment Agency (EEA) [44]. However, the percentage classifications of the water use index to categorize water stress differ in the literature. According to the EEA, a WEI below 10% signifies no water stress, between 10% and 20%, low stress, and greater than 20%, stress. Others, like the World Resources Institute (WRI) [45] and Wang et al. [46] use different classifications. Whereas the WRI

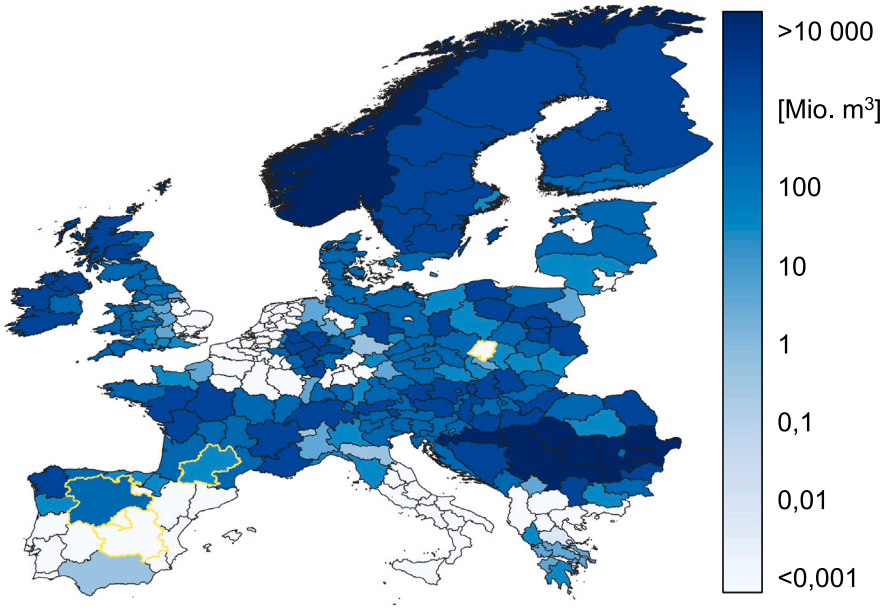

Fig. 4. Availability of fresh water per considered region (notable regions highlighted).

differentiates between low water stress (WEI < 5%), low–medium (5%–25%), medium–high (25%–50%), high (50%–75%), and extremely high (> 75%), Wang et al. extend the scaling to low water scarcity (WEI < 10%), moderate water scarcity (10%–20%), water scarcity (20%–40%), and severe water scarcity (> 40%). According to these classifications, regions with a WEI above 20% are already experiencing water scarcity and are facing water stress problems, e.g., due to excessive water uses such as industrial or agricultural water consumption [44–46]. Additional water consumption by electrolysis plants would only aggravate water stress in these regions leading to severe negative ecological, economical, and social consequences [33–35,44,47]. Hence, in this paper, we assume no freshwater availability for electrolysis in regions with a WEI above 20%.

3. Methods

As Section 2 underlines the development and importance of water in Europe, the following section aims to present an approach to include water in ESOMs. As hydrogen plays a pivotal role in the future multi-energy system and the production process via electrolysis requires water, the importance of water availability in the energy system will strongly increase. To our knowledge, no ESOM has integrated water so far, and so we present an approach to include water availability and water as input for electrolysis within ESOMs and investigate its impact on future energy systems.

The ESOM used for this study is an existing model described by Schwaeppe et al. in [48,49], as well as by Walter et al. in [50,51]. However, a concise explanation of the model, its structure, and its most important constraints, will be given in the following. For further formulation, we refer to the aforementioned sources. The model is a purely linear optimization model with the objective of minimizing investment and dispatch costs. The linearity was chosen to reduce mathematical complexity and thus improve performance. Non-linear relations have therefore been linearized, or neglected, such as the ramp-up constraints of thermal power plants. Additional tables describing sets, variables, and parameters of the model can be found in Appendix.

Fig. 2 shows the technological system overview. The model contains four different energy carriers, namely electricity, hydrogen, methane, and liquid fuels. Electricity from renewable sources is likely to be the main energy carrier in future energy system, with hydrogen based on water and electricity [29]. Methane and liquid fuels as hydrogen derivatives are additional energy carriers included in many scenarios [52]. The modeled infrastructures for these energy carriers consist of the sector-integrating technologies between the energy carriers and their respective transport networks.

The model's objective is the minimization of all systemic costs, more specifically investment and dispatch costs (see. Eq. (1)).

$$\min\ C = C_{CAPEX} + C_{OPEX} \tag{1}$$

The investment costs can be split up for the installation of considered technologies I and increase proportionally to the installed capacity. The investment expenditures are described as annual costs to compare the investment and other costs accumulated throughout the course of a year. The annuity considers the lifetime of the technology $i \in I$ and an interest rate. The total investment costs are the sum of all extended capacities over all plant technologies and nodes, all extended power transfer capacities, and all extended transfer connections of all considered fuels (see. Eq. (2)).

$$C_{CAPEX} = \underbrace{\sum_{i\in I}\sum_{n\in N}(C_i^c \cdot y_{i,n})}_{\text{plant capacities}} + \underbrace{\sum_{e\in E} C_e^{exp}\cdot f_e^{+}}_{\text{power transfer capacities}} + \underbrace{\sum_{q\in Q_{grid}}\sum_{l\in L(q)}(C_l^{q,exp}\cdot f_l^{q,+})}_{\text{fuel transfer capacities}} \tag{2}$$

The dispatch costs contain costs for the generation and storage of electricity, import, the production or storage of fuels, and the utilization of transport infrastructure. The costs are the sum of all technologies, nodes, and time steps (see. Eq. (3)).

$$C_{OPEX} = \sum_{n\in N}\sum_{t\in T}\Bigg(\underbrace{\sum_{i\in I_{EL}} C_i^p \cdot x_{i,n,t}}_{\text{electricity}} + \underbrace{\sum_{e\in E} C_e^{flow}\cdot|f_{e,t}|}_{\text{electricity transport}} + \underbrace{\sum_{i\in I_{FU}}\sum_{q\in Q_{grid}} C_i^p\cdot b_{i,n,t}^q + \sum_{q\in Q_{grid}} C_q\cdot h_{n,t}^q}_{\text{fuels}} + \underbrace{\sum_{q\in Q_{grid}}\sum_{l\in L(q)} C_l^q\cdot|f_{l,t}^q|}_{\text{fuel transport}}\Bigg) \tag{3}$$

The model contains a CO_2 emission limit to consider climate ambitions (see. Eq. (4)). The total emissions are limited by a global

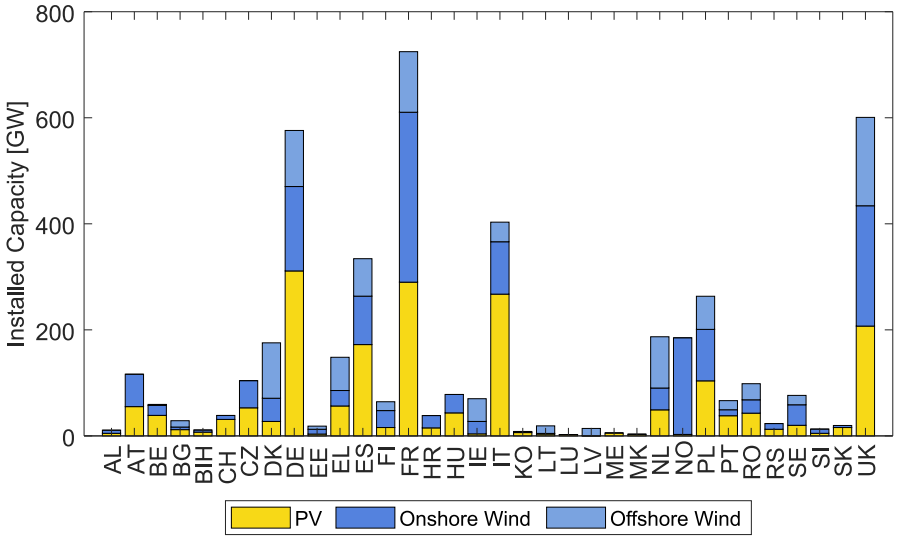

(a) Reference Scenario

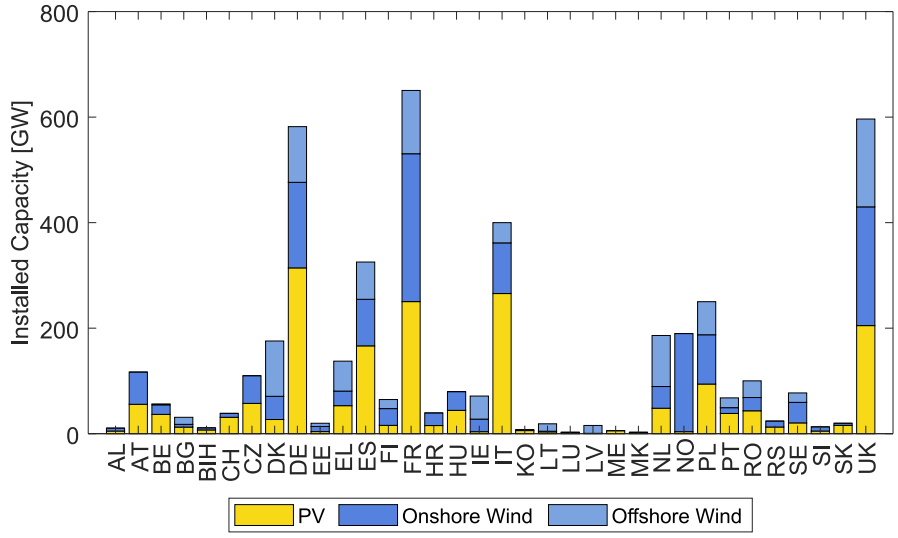

(b) Water Scenario

Fig. 5. Installed capacities of renewable energy sources per country in 2050.

maximum E_{max}. We assess two types of emissions. Emissions of fuels to operate conventional power plants E_i^{op} and emissions from fuels used to cover final energy demand E_q.

$$\sum_{n\in N}\sum_{t\in T}\left(\sum_{i\in I_{EL}} E_i^{op}\cdot x_{i,n,t} + \sum_{q\in Q_{grid}} E^q\cdot h_{n,t}^q\right) \le E_{max} \tag{4}$$

In the following, we will focus on the constraints and variables used for hydrogen production and then present our approach incorporating water availability, water processing, and water as an input for electrolysis.

Electrolysis is part of the set of conversion plants I_{CV} and is modeled as a dispatchable asset with minimum and maximum outputs (see. Eq. (6)). The hydrogen production $b_{i,n,t}^q$ cannot exceed the respective installed electrolysis capacity on node n. The installed capacity is the sum of the initially existing capacities $Y_{i,n}^{init}$ at node n and the extended capacity $y_{i,n}$.

$$0 \le b_{i,n,t}^q \le Y_{i,n}^{init} + y_{i,n} \quad \forall\, i\in I_{CV}, t\in T, n\in N, q\in Out(i) \tag{5}$$

The conversion of electricity into hydrogen is modeled in most ESOMs as is shown in Eq. (6). It depends on the respective efficiency $\eta_i^{q,out}$ with hydrogen being part of the set of fuels Out.

$$b_{i,n,t}^q = \eta_i^{q,out}\cdot x_{i,n,t} \quad \forall\, i\in I_{CV}, t\in T, n\in N, q\in Out(i) \tag{6}$$

Our approach incorporates water availability, water processing, and water as an input for electrolysis, as shown in Fig. 3. Following the analysis in Section 2, we model surface water and seawater as primary water sources and RO as the water processing method. Because the composition of the water sources differs, and thus processing seawater is more energy intensive, a separate osmosis process is modeled for each of the sources with its own efficiency. The resulting clean water is subsequently the input for the electrolysis.

Water extraction pw is limited by the availability of primary water sources PW and is mathematically modeled as a limit per node n (see. Eq. (7)).

$$\sum_t pw_{n,t}^q \le PW_n^{q,max} \quad \forall\, n\in N, t\in T, q\in\{\text{surface water, seawater}\} \tag{7}$$

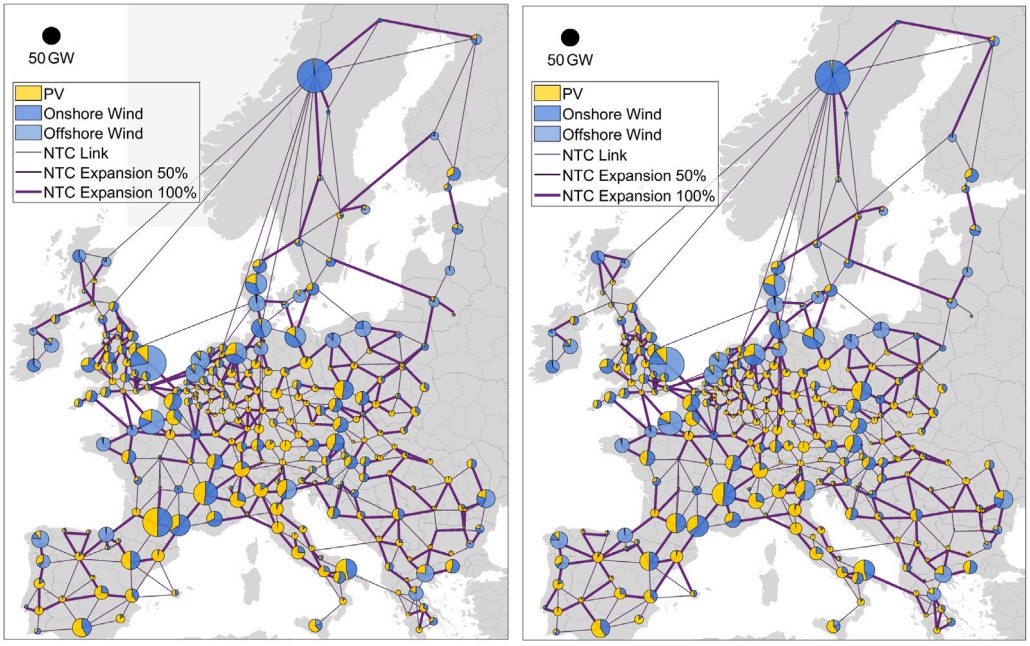

(a) Reference Scenario (b) Water Scenario

Fig. 6. Electric expansion Europe 2050.

To obtain clean water that can be used as an input for electrolysis, the water extracted from primary water sources requires further processing. For each modeled water source, freshwater from surface water and seawater, in this paper, different efficiencies for RO depending on the water source were applied to produce clean water $b_{i,n,t}^{clean\ water}$ for electrolysis.

The production of clean water $b_{i,n,t}^{clean\ water}$ via RO is modeled by the different efficiencies of RO for surface water and seawater (see. Eq. (8)).

$$b_{i,n,t}^{clean\ water} = \eta_i^q \cdot pw_{n,t}^q \quad \forall\ i \in \{RO_{surface}, RO_{sea}\}, t \in T, n \in N, \\ q \in \{\text{surface water, seawater}\} \tag{8}$$

The amount of water processed is limited by the respective installed reverse osmosis capacity $y_{i,n,t}$ (see. Eq. (9)).

$$b_{i,n,t}^{clean\ water} \leq y_{i,n,t} \quad \forall\ i \in \{RO_{surface}, RO_{sea}\}, n \in N, t \in T \tag{9}$$

As a result, two constraints emerge on the modeling of hydrogen production $b_{i,n,t}^q$. One describes the use of electricity $x_{i,n,t}$ and the respective electrical efficiency $\eta_i^{q,el}$ (see. Eq. (10)), and the other constraint describes the input of clean water $b_{i,n,t}^{clean\ water}$ with its respective efficiency η_i^{q,h_2o} (see. Eq. (11)). Mathematically this results in:

$$b_{i,n,t}^q = \eta_i^{q,el} \cdot x_{i,n,t} \quad \forall\ i \in \{electrolysis\}, t \in T, n \in N, q \in \{hydrogen\} \tag{10}$$

and

$$b_{i,n,t}^q = \eta_i^{q,h_2o} \cdot b_{i,n,t}^{clean\ water} \\ \forall\ i \in \{electrolysis\}, t \in T, n \in N, q \in \{hydrogen\} \tag{11}$$

4. Results

In this section, we demonstrate the influence of water availability, reverse osmosis, and water demand for electrolysis on the results of our energy system optimization model. For this purpose, we investigate two scenarios for the target year 2050. One of the scenarios is the Reference Scenario without modeling water processing, and the other is the Water Scenario modeling the availability limits for freshwater and seawater, the water processing via reverse osmosis, and water as an input for electrolysis. Both scenarios share a common data basis and only differ in their consideration of water. Consequently, the temporal, spatial, and techno-economic parameters remain equal in both scenarios.

4.1. Scenario description

The temporal scope of observation is 2050, with a temporal resolution of 8760 h, each hour being a time step. The spatial scope of observation is Europe, including the EU, UK, Norway, Switzerland, and the Balkan states. While the spatial resolution for the EU and the UK is on a NUTS-2 level, we selected a country-level resolution due to data availability for Norway, Switzerland, and the Balkan states. The NUTS-2 level allows excellent spatial coverage while maintaining a computable problem size.

In the scenarios, we include plant and transport infrastructures and the demand for energy carriers such as electricity, hydrogen, methane, and liquid fuels. Input data for demand for these energy carriers is derived from the entso-e TYNDP 2022 scenario, 'Global Ambition' [52]. The final energy demand in our system area for electricity amounts to 4631 TWh, for hydrogen to 2384 TWh, for methane to 1638 TWh, and for liquid fuels to 1135 TWh. We regionalize the total demand volumes by using indicators such as employee numbers, population data, or number of vehicles based on [53–55]. Load profiles and time series from the Energy Transition Model are used for each energy carrier [56]. With regard to input data for the supply side, we use technical potential capacities for wind turbines and PV plants from [57] to model NUTS-2-specific potentials for the expansion of these RES capacities. Feed-in time series for RES were taken from EMHIRES [58,59]. The underlying weather year to which the demand and supply time series correspond is 2012. Further inputs to the model are initial transport infrastructures for electricity, methane, hydrogen, and fuels. For electricity and methane, the transport infrastructure is based on the entso-e respective entsog transmission system [60,61]. The basis for the hydrogen grid is the methane grid without any capacities on connections. For the fuel transport infrastructure, we consider OpenStreetMap data for the road transport network with unlimited capacities on connections [62]. We further apply a network reduction referring to Walter et al. [63], and Frysztacki et al. [20], to provide NUTS-2 level grids. Imports

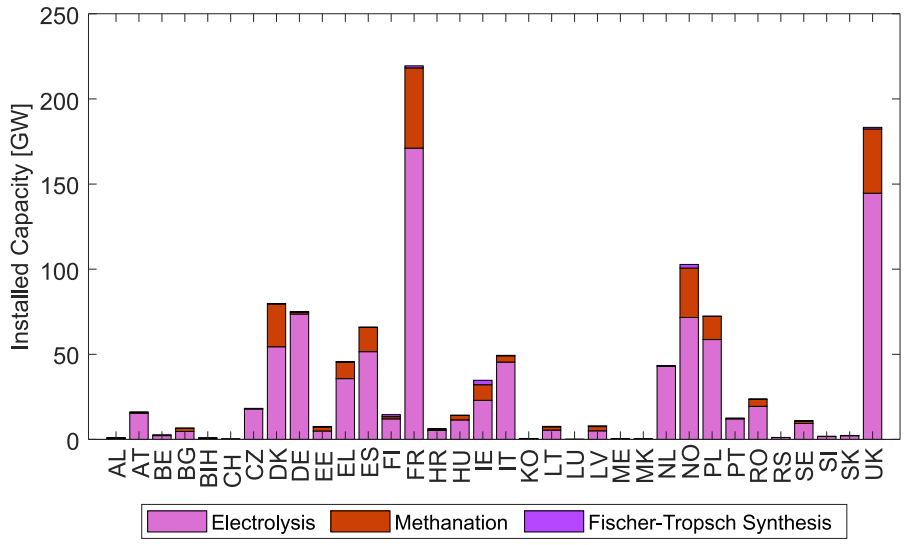

(a) Reference Scenario

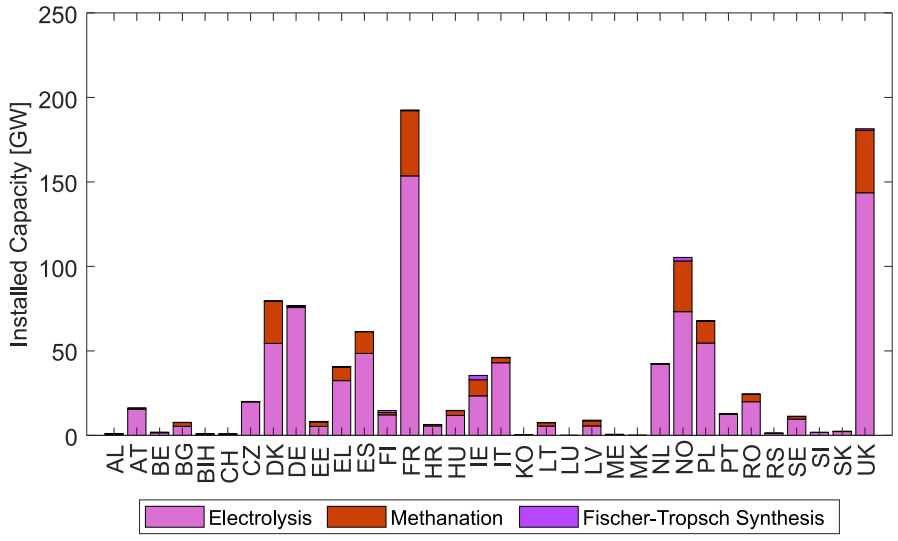

(b) Water Scenario

Fig. 7. Installed power-to-x capacities per country in 2050.

to the system area are possible for hydrogen, methane, and fuels at defined import locations and up to specific import capacities from Gas Infrastructure Europe [64], the Global Energy Observatory [65], and the European Commission [66]. We use a weighted average of country-specific import costs from the PtX Global Atlas from Fraunhofer IEE [67] to consider energy carrier-specific import prices to the EU.

We assign techno-economic parameters to the plant and transport infrastructure based on a database from the Danish Energy Agency [68] and Ram et al. [9]. The interest rate for the annuities is based on historical data from OECD and set to 4.5% [69].

The Reference Scenario is based on the assumption of unlimited and free water availability in all regions. The Water Scenario reflects limited access and the costs of fresh water as a feedstock for electrolysis. Apart from that, it is equal to the Reference Scenario. In the latter, freshwater availability is limited to a WEI of 20% that is below the limit of water stress (see. Section 2). The availability of freshwater is derived from the Aqueduct by the World Resource Institute in 2019 [45,70]. The freshwater consumption by humans is deducted and Fig. 4 shows the resulting amounts of water available per region for electrolysis. We further assume that coastal regions have access to fresh water through water processing via reverse osmosis. The potential for this is unlimited but attached to investment and operational costs.

4.2. Results

To show the effect of considering water as a limited, more precise geographically limited input for electrolysis on the results of ESOMs, we compare the most important results, such as installed capacities and the locations of RES, electrolysis, methanation, and Fischer–Tropsch (FT) plants, side-by-side.

The installed capacities of RES and the resulting technology mix do not change substantially in total between the Reference Scenario and the Water Scenario (see. Figs. 5 and 6). In the Water Scenario, there is about 87.7 GW less total installed capacity of RES. This is about a 2% difference, with an overall installed RES capacity of around 4588 GW in the Reference Scenario and 4500 GW in the Water one. While for PV and onshore wind, there is a decrease of about 52 GW respective 44 GW, the total installed capacity of offshore wind increases by about 8.2 GW. The increase in offshore wind capacities indicates a shift from electrolyzer capacities from inland to coastal regions.

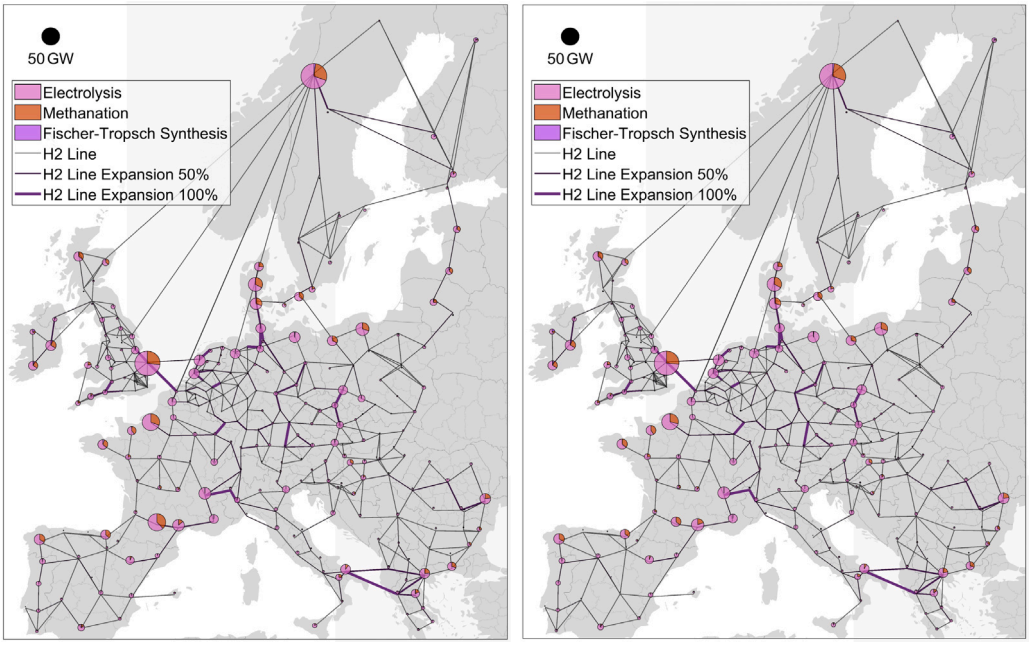

(a) Reference Scenario (b) Water Scenario

Fig. 8. Synthetic fuel expansion Europe in 2050.

Table 1
Installed power-to-x capacities per scenario in GW.

	Reference Scenario	Water Scenario	Difference
Electrolysis	906.4	883.5	−22.9
Methanation	211.5	200.3	−11.2
Fischer–Tropsch	11.7	10.4	−1.3

The most significant numbers of installed RES capacities are in France, Germany, and the UK. Comparing the installed capacities per country (see. Fig. 5), the results show the most significant change in installed RES capacities in France. By numbers, in the Reference Scenario in France, there are 289 GW of PV, 320 GW of onshore wind, and 114 GW of offshore wind (see. Fig. 5(a)). In the Water Scenario, these numbers decrease to 250 GW of PV, 280 GW of onshore wind, and an increase of offshore wind to 120 GW (see. Fig. 5(b)).

The amount of installed capacities of RES in some regions changes significantly, though (see. Fig. 6). The Midi-Pyrénées (FRJ2) region in the south-western France, e.g., experiences not only the overall highest decrease of PV but also of onshore wind with 36 GW and 37 GW, resulting in the total RES capacity in FRJ2 to be more than halved. Another salient change when considering water availability is in the Opole Voivodeship (PL52) in Poland. There, the installed RES capacity is halved, and in absolute terms, the installed PV capacity decreases by 11.7 GW and the onshore wind capacity by 5.5 GW.

A noticeable shift of RES capacity from one region to another is apparent between the two scenarios in Spain. The Castilla-La-Mancha (ES42) region records little water availability. Its neighboring region of Castilla *y* León (ES41) does, however. The decrease in the Water Scenario of RES capacity of about 9 GW in ES42 and the increase of about 5.1 GW indicates a relocation from electrolysis due to water availability limits (see. Fig. 4).

The total installed Power-to-X (PtX) capacities in the scenarios do not change significantly (see. Table 1). The relative decrease in total installed electrolysis capacity between the two scenarios is about 2.5%, the methanation capacities decrease by about 5.2%, and the FT capacities by about 11%.

In both scenarios, most electrolysis capacities are installed in France (see. Fig. 7) with 171.1 GW in the Reference Scenario and 153.6 GW in the Water one. France is followed by the UK, and with a distance, by Germany and Norway in terms of installed electrolysis capacity. France experiences the highest decrease in electrolysis capacity, with about 17.5 GW. While countries like Poland (−4 GW) and Spain (−3.2 GW) see a decrease in electrolysis capacity from the Reference to the Water Scenario, ones like Germany (+ 2 GW), the Czech Republic (+ 1.9 GW), and Norway (+ 1.6 GW) see an increase.

Most countries with large installed electrolysis capacities also expand methanation capacities in both scenarios. For example, Denmark must be highlighted because its installed electrolysis capacity is lower than Germany's, but the overall installed PtX capacities are higher than Germany's (see. Fig. 7). This implies that Denmark and others can exceed their hydrogen demand and use the hydrogen surplus to synthesize methane. The highest methanation capacities are located in France, followed by the UK and Norway (see. Fig. 7). The largest decreases in methanation capacities between both scenarios are linked to the decreases in electrolysis capacities. France, with a decrease of about 8.5 GW, Greece with 1.7 GW, and Spain with 1.4 GW (see. Fig. 7).

In comparison to electrolysis and methanation, only a few Fischer–Tropsch capacities are installed in both scenarios (see. Table 1 and Fig. 7), most of them in Ireland and Norway.

The aforementioned regions, in which high decreases in RES capacity occur by including water as input for electrolysis and introducing limited freshwater availability, are the same regions to have the highest change in installed electrolysis capacity: FRJ2 with about −20.2 GW, PL52 with −7.5 GW, and ES42 with −3 GW (see. Fig. 8). The results show that large parts of the electrolysis capacities are being relocated to neighboring regions with freshwater access or, to a lesser extent, with saltwater access due to the limited availability of water. The results of the Spanish region ES42 show the typical relocation of electrolysis capacities as in the neighboring region ES41, where the installed capacity of electrolysis increased by about 1.8 GW.

The decrease and relocation of electrolysis capacities cause a small change in synthetic hydrogen imports from the outside of the system area. Almost all of the hydrogen demand is domestically covered, and only 89 GWh in the reference scenario and 137 GWh are imported from outside of Europe. As already noted, the change in electrolysis capacities influences the decrease of methanation capacities and, subsequently, the import of synthetic methane from outside Europe. The

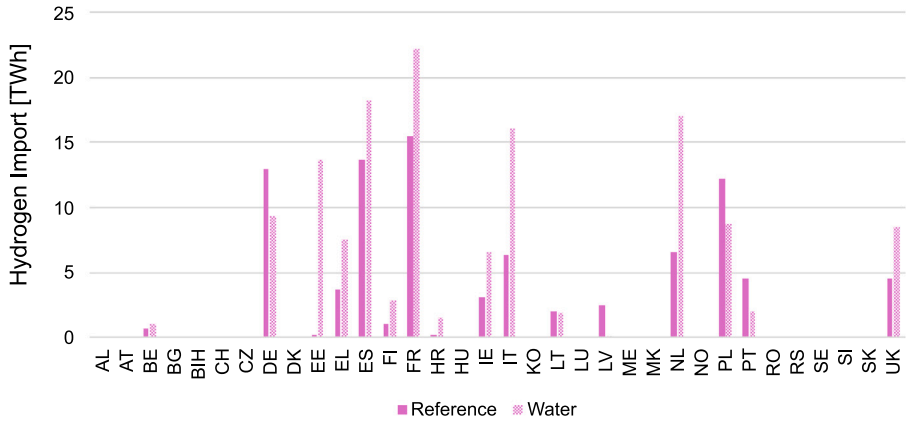

(a) Synthetic hydrogen import

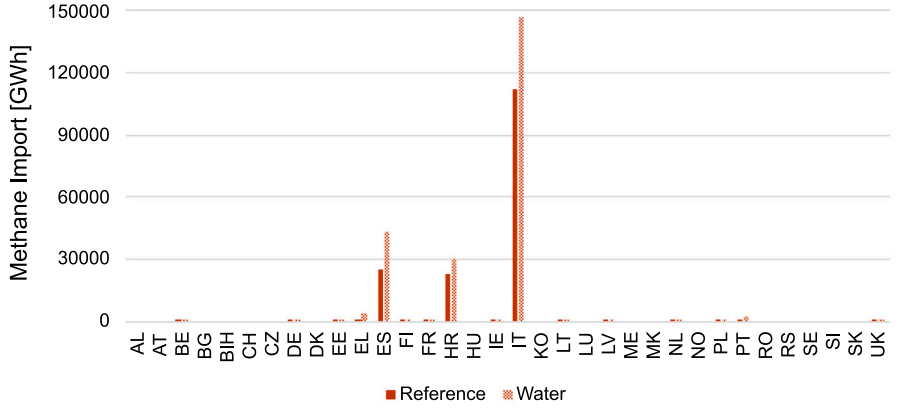

(b) Synthetic methane import

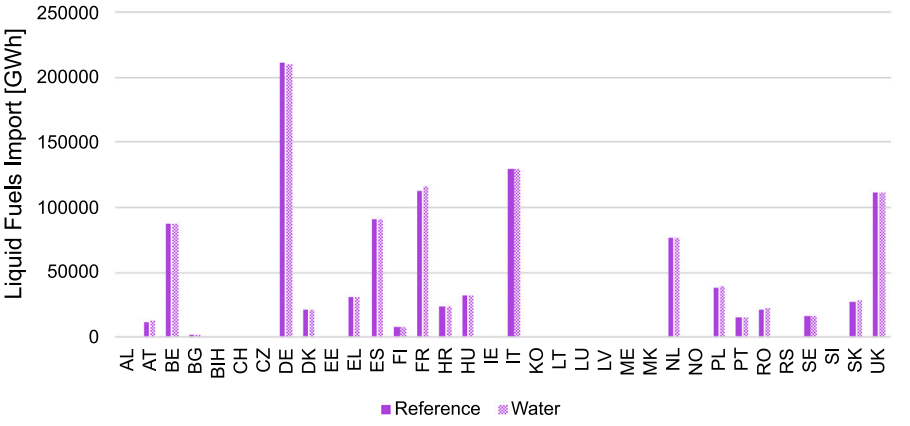

(c) Synthetic liquid fuels import

Fig. 9. Synthetic fuels import from outside the geographic system area.

imports of synthetic methane increase about 40% up to 226 TWh, which is about 14% of the final methane demand. The import of liquid fuels changes between the scenarios by less than 1%. In relation to the final energy demand, the imports amount to less than 0.06% for hydrogen, between 10% and 14% for methane, and about 94% for liquid fuels in both scenarios (see. Fig. 9). This further underlines the effect on decreased methanation capacities and synthetic methane production due to lower electrolysis capacities in the Water Scenario. Considering water as a relevant and limited factor leads to a higher import dependency not only for hydrogen but also for synthetic methane because of the lower amount of domestically produced hydrogen. The greater change in imports of synthetic methane in comparison to synthetic liquid fuels underscores not only the direct link between electrolysis capacities and methanation capacities but also the higher energetic efficiency of the synthesis of methane from hydrogen rather than liquid fuels through Fischer–Tropsch as parameterized.

The total decrease of electrolysis capacity in the Water Scenario in comparison to the Reference one is about 23 GW, but the total relocation of electrolysis capacities is 100 GW, which is more than 10% of the installed electrolysis capacities. Fig. 10 displays the percentage change of electrolysis capacities between the Reference Scenario and Water one. Implementing water availability (see. Fig. 4) results in

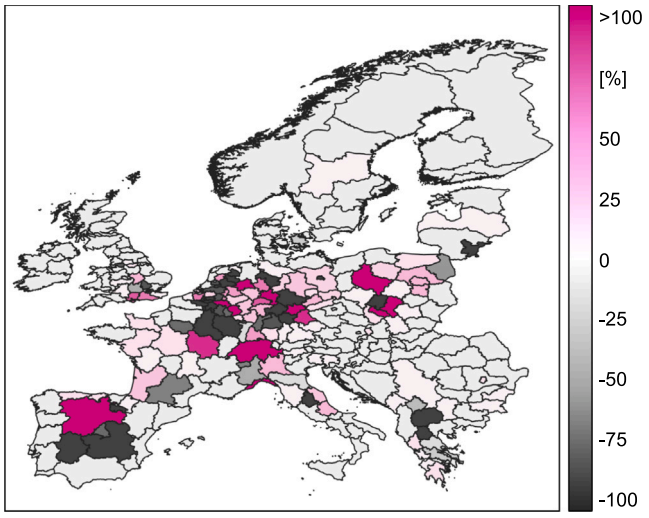

Fig. 10. Change in electrolyzer capacities.

different electrolysis capacity locations. In most cases, the capacities move to neighboring regions with fresh water availability, as in the aforementioned and Fig. 4 in the highlighted regions. For some capacities, as in central Italy, the electrolysis capacities are relocated to neighboring regions on the coast in order to use seawater and reverse osmosis to prepare water for electrolysis.

5. Discussion and conclusion

In order to mitigate climate change and achieve the European climate goals, a transition towards a sector-integrated energy system is necessary. Within the sector-integrated energy system, hydrogen-based on electricity from RES and water will play a pivotal role as the final energy carrier or interim step for producing hydrocarbons like methane or FT-fuels. While the effect of the RES and additional capacities has been investigated in many studies, the effect of limited water availability, with water from seawater, water processing, and water as input for hydrogen production in electrolysis, respectively, on the design of the future multi-energy system is, to our knowledge, a novelty provided by this study. In the future energy system, the efficient utilization of resources will be a crucial challenge and fresh water will be less and less available as a regional resource. This prompted the research questions of how to model water availability in ESOMs and, in particular, to what extent water affects future energy system design.

We implemented regional freshwater availability as limits in our model, water processing from fresh and seawater with different efficiencies via reverse osmosis, and considered water as a necessary input for producing hydrogen into an existing ESOM. The findings showed that the consideration of water strongly influences the total and regional amount of not only electrolysis capacities but also methanation and FT plants. The overall relocation of electrolysis capacities is about 10% compared to the one that does not consider water. Furthermore, substantial effects on methane imports to Europe could be derived from the investigated scenario. The decline and relocation of electrolysis capacities also led to a decrease in methanation capacities and an increase of about 40% in methane imports. This implicates a rise in European energy import dependency because of the lower amount of domestically produced hydrogen.

Although the linear optimization model may not fully capture all patterns that affect the input for electrolysis within ESOMs, it provides reasonable trends in energy system planning. Taken together, our findings demonstrate that the study's high temporal and spatial resolution and the implementation of interactions between the energy sectors of electricity, hydrogen, methane, and FT-fuels are advantageous for the accuracy and interpretability of the results. Hence, we were able to show that electrolysis capacities relocate to neighboring regions with remaining water availability and/or coastal regions for seawater processing when considering water availability and water as input for electrolysis.

Despite being based on a single scenario, our findings demonstrate the profound impact of integrating water availability, reverse osmosis, and water as an input for electrolysis into ESOMs investigating the future European energy system. Water scarcity or abundance significantly influences not only energy system planning but also social, ecological, economic, and sanitary aspects. This study emphasizes the necessity of incorporating water availability into energy system planning to develop comprehensive and sustainable strategies. Neglecting water constraints could lead to suboptimal energy policies, resulting in detrimental effects in other sectors.

Having shown the interdependencies between water and energy system design, it is imperative that future research and energy system optimization models integrate water availability as a constraint. The magnitude of water's impact may vary under different scenarios, import prices, investment costs, or regional water availability data. Therefore, expanding the scope of analysis to encompass a broader range of scenarios is essential to understanding and addressing these complexities fully. Expanding the scope may also imply addressing the interactions between water and biomass, another renewable but limited resource, that is important for the transition to a climate-neutral and sector-integrated European energy system.

This study clearly shows that integrating water availability constraints is not only beneficial but essential for robust scenario development in policymaking and strategic planning by energy supply companies in the process of identifying electrolysis sites, as well as electricity and gas grid operators. Incorporating water constraints ensures the development of resilient and sustainable energy systems capable of meeting future demands without negatively affecting other critical sectors. We strongly recommend the inclusion of water availability in energy system optimization models to ensure that future energy strategies and energy system designs are both feasible and resilient while ensuring social, ecological, economic, and sanitary interests.

CRediT authorship contribution statement

Julian Walter: Writing – original draft, Visualization, Validation, Software, Resources, Methodology, Investigation, Formal analysis, Data curation, Conceptualization. **Lina Fischer:** Writing – review & editing, Visualization, Validation, Software, Resources, Methodology, Investigation, Formal analysis, Data curation, Conceptualization. **Sandra Venghaus:** Writing – review & editing, Supervision. **Albert Moser:** Supervision, Project administration, Funding acquisition.

Declaration of competing interest

The authors declare that they have no known competing financial interests or personal relationships that could have appeared to influence the work reported in this paper.

Acknowledgments

Funded by the Deutsche Forschungsgemeinschaft (DFG, German Research Foundation) under Germany's Excellence Strategy – Exzellenzcluster 2186 "The Fuel Science Center" ID: 390919832.

Appendix

See Tables 2–5.

Data availability

Data will be made available on request.

Table 2
Relevant indices and sets of the ESOM.

Set	Description
$i \in I$	Technologies
$n \in N$	Nodes
$q \in Q$	Fuels
$e \in E$	Power transfer connections
$l \in L$	Fuel transfer connections
$t \in T$	Time steps

Table 3
Relevant subsets of the ESOM.

Set	Description
$Q_{grid} \subseteq Q$	Fuels with transport network
$Q_{water} \subseteq Q$	Water sources
$L(q) \subseteq L$	Transport connections for fuel type q
$In(i) \subseteq Q$	Fuels which are input of technology i
$Out(i) \subseteq Q$	Fuels which are output of technology i
$I_{EL} \subseteq I$	Technologies which generate or store electricity
$I_{FU} \subseteq I$	Technologies that generate or store fuels
$I_{CV} \subseteq I_{FU}$	Energy conversion technologies
$I_{Water} \subseteq I$	Reverse osmosis processing plants

Table 4
Relevant variables of the ESOM.

Variable	Description
$x_{i,n,t}$	Injection/withdrawal of electricity by technology i at node n in time step t
$y_{i,n}$	Additional installed capacity of technology i at node n
$f_{e,t}$	Power flow across connection e in time step t
f_e^+	Capacity expansion of power transfer connection e
$f_{l,t}^q$	Flow of fuel q across connection l in time step t
$f_l^{q,+}$	Capacity expansion of fuel transfer connection l for fuel q
$b_{i,n,t}^q$	Injection/withdrawal of fuel q at node n in time step t
$h_{n,t}^q$	Import of fuel q at node n in time step t

Table 5
Relevant parameters of the ESOM.

Symbol	Description
C_i^p	Annual investment costs of a technology i
C_i^c	Annuity costs for the expansion of technology i per unit
C_e^{exp}	Annuity costs for the capacity expansion of power transfer connection e per unit
$C_l^{q,exp}$	Annuity costs for capacity expansion of fuel transfer connection l for fuel q per unit
C_e^{flow}	Costs per unit of power flow across connection e
C_l^q	Costs per unit of flow from fuel q across connection l
C_q	(Import) costs per unit of fuel q
E_{max}	Global emission maximum
E_i^{op}	Emissions of operation from technology i per unit
E_q	Emissions of imported fuel q per unit
$Y_{i,n}^{init}$	Initially installed capacity of technology i at node n
$\eta_i^{q,in}, \eta_i^{q,out}$	Efficiency of technology i for conversion of/to fuel q

References

[1] United Nations. The Paris Agreement. 2015, URL https://unfccc.int/process-and-meetings/the-paris-agreement.

[2] European Commission. In: European Commission, editor. The European green deal. 2019, URL https://commission.europa.eu/strategy-and-policy/priorities-2019-2024/european-green-deal_en.

[3] Schreyer F, Ueckerdt F, Pietzcker R, Rodrigues R, Rottoli M, Madeddu S, et al. Distinct roles of direct and indirect electrification in pathways to a renewables-dominated European energy system. One Earth 2024;7(2):226–41. http://dx.doi.org/10.1016/j.oneear.2024.01.015.

[4] Bogdanov D, Ram M, Khalili S, Aghahosseini A, Fasihi M, Breyer C. Effects of direct and indirect electrification on transport energy demand during the energy transition. Energy Policy 2024;192:114205. http://dx.doi.org/10.1016/j.enpol.2024.114205.

[5] Sorknæs P, Johannsen RM, Korberg AD, Nielsen TB, Petersen UR, Mathiesen BV. Electrification of the industrial sector in 100% renewable energy scenarios. Energy 2022;254:124339. http://dx.doi.org/10.1016/j.energy.2022.124339.

[6] Béres R, Nijs W, Boldrini A, van den Broek M. Will hydrogen and synthetic fuels energize our future? Their role in Europe's climate-neutral energy system and power system dynamics. Appl Energy 2024;375:124053. http://dx.doi.org/10.1016/j.apenergy.2024.124053.

[7] Cao S, Li Y, Tang Y, Sun Y, Li W, Guo X, et al. Space-confined metal ion strategy for carbon materials derived from cobalt benzimidazole frameworks with high desalination performance in simulated seawater. Adv Mater (Deerfield Beach, Fla) 2023;35(23):e2301011. http://dx.doi.org/10.1002/adma.202301011.

[8] Su L, Wu H, Zhang S, Cui C, Zhou S, Pang H. Insight into intermediate behaviors and design strategies of platinum group metal-based alkaline hydrogen oxidation catalysts. Adv Mater (Deerfield Beach, Fla) 2024;e2414628. http://dx.doi.org/10.1002/adma.202414628.

[9] Ram M, Galimova T, Bogdanov D, Fasihi M, Gulagi. Powerfuels in a renewable energy world. 2020, URL https://www.powerfuels.org/fileadmin/powerfuels.org/Dokumente/Global_Alliance_Powerfuels_Study_Powerfuels_in_a_Renewable_Energy_World.pdf.

[10] Blanco H, Nijs W, Ruf J, Faaij A. Potential for hydrogen and power-to-liquid in a low-carbon EU energy system using cost optimization. Appl Energy 2018;232:617–39. http://dx.doi.org/10.1016/j.apenergy.2018.09.216.

[11] European Commission. In: European Commission, editor. A hydrogen strategy for a climate-neutral Europe. Brussels; 2020, URL https://eur-lex.europa.eu/legal-content/EN/TXT/?uri=CELEX:52020DC0301.

[12] Prina MG, Manzolini G, Moser D, Nastasi B, Sparber W. Classification and challenges of bottom-up energy system models - A review. Renew Sustain Energy Rev 2020;129:109917. http://dx.doi.org/10.1016/j.rser.2020.109917.

[13] Lopion P, Markewitz P, Robinius M, Stolten D. A review of current challenges and trends in energy systems modeling. Renew Sustain Energy Rev 2018;96:156–66. http://dx.doi.org/10.1016/j.rser.2018.07.045.

[14] Wiese F, Bramstoft R, Koduvere H, Pizarro Alonso A, Balyk O, Kirkerud JG, et al. Balmorel open source energy system model. Energy Strategy Rev 2018;20:26–34. http://dx.doi.org/10.1016/j.esr.2018.01.003.

[15] Hörsch J, Hofmann F, Schlachtberger D, Brown T. PyPSA-Eur: An open optimisation model of the European transmission system. Energy Strategy Rev 2018;22:207–15. http://dx.doi.org/10.1016/j.esr.2018.08.012.

[16] Löffler K, Hainsch K, Burandt T, Oei P-Y, Kemfert C, von Hirschhausen C. Designing a model for the global energy system—GENeSYS-MOD: An application of the open-source energy modeling system (OSeMOSYS). Energies 2017;10(10):1468. http://dx.doi.org/10.3390/en10101468.

[17] Hoffmann M, Kotzur L, Stolten D, Robinius M. A review on time series aggregation methods for energy system models. Energies 2020;13(3):641. http://dx.doi.org/10.3390/en13030641.

[18] Prina MG, Casalicchio V, Kaldemeyer C, Manzolini G, Moser D, Wanitschke A, et al. Multi-objective investment optimization for energy system models in high temporal and spatial resolution. Appl Energy 2020;264:114728. http://dx.doi.org/10.1016/j.apenergy.2020.114728, URL https://www.sciencedirect.com/science/article/pii/S0306261920302403.

[19] Martínez-Gordón R, Morales-España G, Sijm J, Faaij A. A review of the role of spatial resolution in energy systems modelling: Lessons learned and applicability to the North Sea region. Renew Sustain Energy Rev 2021;141:110857. http://dx.doi.org/10.1016/j.rser.2021.110857.

[20] Frysztacki MM, Hörsch J, Hagenmeyer V, Brown T. The strong effect of network resolution on electricity system models with high shares of wind and solar. Appl Energy 2021;291:116726. http://dx.doi.org/10.1016/j.apenergy.2021.116726.

[21] Brown T, Hörsch J, Schlachtberger D. PyPSA: Python for power system analysis. J Open Res Softw 2018;6. http://dx.doi.org/10.5334/jors.188.

[22] Wierzbowski M, Lyzwa W, Musial I. MILP model for long-term energy mix planning with consideration of power system reserves. Appl Energy 2016;169:93–111. http://dx.doi.org/10.1016/j.apenergy.2016.02.003.

[23] E3 Modelling. PRIMES. 2018, URL https://e3modelling.com/modelling-tools/primes/.

[24] Felling T, Levers O, Fortenbacher P. Multi-horizon planning of multi-energy systems. Electr Power Syst Res 2022;212:108509. http://dx.doi.org/10.1016/j.epsr.2022.108509.

[25] Gils HC, Gardian H, Schmugge J. Interaction of hydrogen infrastructures with other sector coupling options towards a zero-emission energy system in Germany. Renew Energy 2021;180:140–56. http://dx.doi.org/10.1016/j.renene.2021.08.016.

[26] Brown T, Schlachtberger D, Kies A, Schramm S, Greiner M. Synergies of sector coupling and transmission reinforcement in a cost-optimised, highly renewable European energy system. Energy 2018;160:720–39. http://dx.doi.org/10.1016/j.energy.2018.06.222.

[27] Wogrin S, Tejada-Arango DA, Gaugl R, Klatzer T, Bachhiesl U. LEGO: The open-source low-carbon expansion generation optimization model. SoftwareX 2022;19:101141. http://dx.doi.org/10.1016/j.softx.2022.101141.

[28] Fodstad M, Del Crespo Granado P, Hellemo L, Knudsen BR, Pisciella P, Silvast A, et al. Next frontiers in energy system modelling: A review on challenges and the state of the art. Renew Sustain Energy Rev 2022;160:112246. http://dx.doi.org/10.1016/j.rser.2022.112246.

[29] Klatzer T, Bachhiesl U, Wogrin S, Tomasgard A. Ramping up the hydrogen sector: An energy system modeling framework. Appl Energy 2024;355:122264. http://dx.doi.org/10.1016/j.apenergy.2023.122264.

[30] Brown T, Schäfer M, Greiner M. Sectoral interactions as carbon dioxide emissions approach zero in a highly-renewable European energy system. Energies 2019;12(6):1032. http://dx.doi.org/10.3390/en12061032.

[31] Luck M, Landis M, Gassert F. Aqueduct water stress projections: Decadal projections of water supply and demand using CMIP5 CGMs: Technical note. World Resource Institute; 2015, URL https://www.wri.org/publication/aqueduct-water-stress-projections.

[32] European Environment Agency. Water Stress URL https://www.eea.europa.eu/help/glossary/eea-glossary/water-stress.

[33] Cordery I. Coping with Water Scarcity: Addressing the Challenges. Dordrecht: Springer Netherlands; 2009, URL https://ebookcentral.proquest.com/lib/kxp/detail.action?docID=428808.

[34] European Climate and Health Observatory. In: European Union, editor. Drought and water scarcity. 2024, URL https://climate-adapt.eea.europa.eu/en/observatory/evidence/health-effects/drought-and-water-scarcity.

[35] Unfried K, Kis-Katos K, Poser T. Water scarcity and social conflict. J Environ Econ Manag 2022;113:102633. http://dx.doi.org/10.1016/j.jeem.2022.102633.

[36] Simoes SG, Catarino J, Picado A, Lopes TF, Di Berardino S, Amorim F, et al. Water availability and water usage solutions for electrolysis in hydrogen production. J Clean Prod 2021;315:128124. http://dx.doi.org/10.1016/j.jclepro.2021.128124.

[37] European Commission and Joint Research Centre, Bisselink B, Bernhard J, Gelati E, Adamovic M, Guenther S, et al. Climate change and Europe's water resources. Publications Office; 2020, http://dx.doi.org/10.2760/15553.

[38] Beswick RR, Oliveira AM, Yan Y. Does the green hydrogen economy have a water problem? ACS Energy Lett 2021;6(9):3167–9. http://dx.doi.org/10.1021/acsenergylett.1c01375.

[39] Water resources across Europe: Confronting water stress : an updated assessment. In: EEA report, no. 2021, 12, Luxembourg: Publications Office of the European Union, European Environment Agency; 2021, http://dx.doi.org/10.2800/320975.

[40] Institute WR. Aqueduct: Using cutting-edge data to identify and evaluate water risks around the world. 2024, URL https://www.wri.org/aqueduct.

[41] Venghaus S, Hake J-F. Nexus thinking in current EU policies – The interdependencies among food, energy and water resources. Environ Sci Policy 2018;90:183–92. http://dx.doi.org/10.1016/j.envsci.2017.12.014.

[42] D'Odorico P, Davis KF, Rosa L, Carr JA, Chiarelli D, Dell'Angelo J, et al. The global food–energy–water nexus. Rev Geophys 2018;56(3):456–531. http://dx.doi.org/10.1029/2017RG000591.

[43] Stephan RM, Mohtar RH, Daher B, Embid Irujo A, Hillers A, Ganter JC, et al. Water–energy–food nexus: a platform for implementing the Sustainable Development Goals. Water Int 2018;43(3):472–9. http://dx.doi.org/10.1080/02508060.2018.1446581.

[44] European Environment Agency. Environment in the European union at the turn of the century: Environmental assessment report No 2. 1999, p. 155.

[45] Hofste R, Kuzma S, Walker S, Sutanudjaja E, Bierkens M, Kuijper M, et al. Aqueduct 3.0: Updated Decision-Relevant Global Water Risk Indicators. World Resources Institute; 2019, http://dx.doi.org/10.46830/writn.18.00146.

[46] Wang D, Hubacek K, Shan Y, Gerbens-Leenes W, Liu J. A review of water stress and water footprint accounting. Water 2021;13(2):201. http://dx.doi.org/10.3390/w13020201, URL https://www.mdpi.com/2073-4441/13/2/201.

[47] Eslamian FA, Eslamian S, editors. Handbook of drought and water scarcity: Principles of drought and water scarcity. New York: CRC Press; 2017, http://dx.doi.org/10.1201/9781315404219, URL https://www.taylorfrancis.com/books/9781315404219.

[48] Schwaeppe H, Moser A, Paronuzzi P, Monaci M. Generation and transmission expansion planning with respect to global warming potential. 2021, http://dx.doi.org/10.36227/techrxiv.14453694.v1.

[49] Schwaeppe H, Böttcher L, Schumann K, Hein L, Hälsig P, Thams S, et al. Analyzing intersectoral benefits of district heating in an integrated generation and transmission expansion planning model. Energies 2022;15(7):2314. http://dx.doi.org/10.3390/en15072314.

[50] Walter J, Goertz S, Inghelram W, Moser A. Application of a multi-horizon multi-energy optimization model for a European case study. In: 2023 IEEE PES innovative smart grid technologies - Asia. IEEE; 2023, p. 1–5. http://dx.doi.org/10.1109/ISGTAsia54891.2023.10372790.

[51] Walter J, Wähner F, Rudolph L, Schwaeppe H, Moser A. Method for the efficient determination of transformation paths for sector-integrated energy systems. In: 2023 international conference on future energy solutions. Piscataway, NJ: IEEE; 2023, p. 1–6. http://dx.doi.org/10.1109/FES57669.2023.10183301.

[52] ENTSOE, ENTSOG. TYNDP scenario report 2022. 2022, URL https://2022.entsos-tyndp-scenarios.eu/.

[53] Eurostat. Beschäftigung nach geschlecht, alter, wirtschaftszweigen und NUTS-2-regionen. 2022, URL https://ec.europa.eu/eurostat/de/web/products-datasets/-/LFST_R_LFE2EN2.

[54] Eurostat. Bestand der Fahrzeuge nach Kategorie und NUTS-2-Regionen. 2023, URL https://data.europa.eu/data/datasets/nhmove15jqyapyxty0rpjw?locale=de.

[55] Eurostat. Bevölkerung am 1. Januar nach NUTS-2-Region. 2023, URL https://data.europa.eu/data/datasets/caxrod4eyvyjuqbmq8vqa?locale=de.

[56] Quintel. Energy transition model. 2023, URL https://energytransitionmodel.com/.

[57] Ruiz P, Nijs W, Tarvydas D, Sgobbi A, Zucker A, Pilli R, et al. ENSPRESO - an open, EU-28 wide, transparent and coherent database of wind, solar and biomass energy potentials. Energy Strategy Rev 2019;26:100379. http://dx.doi.org/10.1016/j.esr.2019.100379.

[58] Gonzalez Aparicio I, Zucker A, Careri F, Monforti Ferrario F, Huld T, Badger J. Wind hourly generation time series at country, NUTS 1, NUTS 2 level and bidding zones. In: EMHIRES: European meteorological derived high resolution rES generation time series for present and future scenarios, 2016, URL https://data.jrc.ec.europa.eu/dataset/jrc-emhires-wind-generation-time-series.

[59] Gonzalez Aparicio I, Huld T, Careri F, Monforti Ferrario F, Zucker A. Solar hourly generation time series at country, NUTS 1, NUTS 2 level and bidding zones. In: EMHIRES: European meteorological derived high resolution rES generation time series for present and future scenarios, 2017, URL http://data.europa.eu/89h/jrc-emhires-solar-generation-time-series.

[60] ENTSOE. Grid Map URL https://www.entsoe.eu/data/map/.

[61] ENTSOG. System capacity map. 2024, URL https://www.entsog.eu/maps.

[62] Open Street Map URL https://www.openstreetmap.org.

[63] Walter JD, Löhr L, Schwaeppe H, Moser A. Network reduction approach for sector-coupled energy system optimization. RWTH Aachen University; 2023, http://dx.doi.org/10.18154/RWTH-2022-09288.

[64] Gas Infrastructure Europe. GIE LNG Database. 2022, URL https://www.gie.eu/transparency/databases/lng-database/.

[65] Global Energy Observatory. Current list of oil ports transmission. 2018, URL https://globalenergyobservatory.org/list.php?db=Transmission&type=Oil_Ports.

[66] Europäische Kommission. Registration of crude oil imports and deliveries in the European union (EU28) (1). 2019.

[67] Frauenhofer IEE. PtX global ATLAS. 2021, URL https://maps.iee.fraunhofer.de/ptx-atlas/.

[68] Danish Energy Agency. Technology data. 2023, URL https://ens.dk/en/our-services/projections-and-models/technology-data.

[69] OECD. Long-term interest rates forecast. 2023, URL https://data.oecd.org/interest/long-term-interest-rates-forecast.htm#indicator-chart.

[70] World Resources Institute. Aqueduct Water Risk Atlas URL https://www.wri.org/aqueduct/tools.